ANALYSIS OF REPAIRED REINFORCED CONCRETE STRUCTURES

By F. J. Vecchio[1] and F. Bucci[2]

ABSTRACT: A procedure is described by which nonlinear finite-element algorithms can be modified to enable the analysis of repaired or rehabilitated concrete structures, taking into account the chronology of the loading, damage, and repair. The method defines and employs plastic strain offsets in the context of a smeared rotating crack model. The ability to engage and disengage elements at various stages of loading, as well as the ability to carry forward strain measures representing previous loading and damage conditions, are key aspects in the analysis method. Analysis of beams and slabs repaired with fiber-reinforced plastics demonstrates the accuracy of the procedure in accounting for changes in strength, stiffness, ductility, and failure mode as a result of strengthening measures. Flexure-dominated and shear-dominated responses are equally well represented. The analysis of a repaired shear wall, subjected to reversed cyclic loads, illustrates the ability to model severely damaged structures where some portions must be removed and reconstructed. In all cases, the analysis procedure was numerically stable and efficient at all stages of loading.

INTRODUCTION

According to some estimates, the money spent in North America on retrofitting existing structures, in recent years, has exceeded that spent on the construction of new facilities. This trend is expected to intensify, as infrastructure continues to age. Compounding the situation are several other factors. First, design codes today are generally more stringent than those effective at the time of first construction, particularly with respect to out-of-plane shear design and earthquake-resistant design. In addition, governments have entered an era of financial restraint and austerity and are less inclined to expend public funds on new construction if avoidable.

In reaction to this trend, much of the recent research relating to concrete structures has been in the area of rehabilitation and repair. This activity, however, has been primarily concerned with developing effective repair materials and techniques, such as using fiber-reinforced plastic (FRP) wraps or external prestressing. Related research has also been undertaken to experimentally observe the influence that various repair materials have on the overall behavior, strength, and ductility of typical structural elements. Lagging behind, however, has been complementary work in developing analysis techniques that enable a rigorous representation of the performance and safety of repaired structures, or a rational assessment of different repair scenarios.

From an analysis perspective, a rigorous quantitative assessment of a repaired or rehabilitated concrete structure presents a formidable challenge. Extensive reformulation of nonlinear algorithms is required to enable the following: consideration of changing structural configuration; superposition of previously loaded or damaged portions of a structure with newly-added unstressed elements; proper constitutive modeling of the repair materials; and inclusion of residual stresses and strain differentials across repair interfaces. Further, correct account must be made of the chronology of the loading, damage, and repair sequences.

Previous work on theoretical modeling of repaired structures has been largely sporadic and limited in scope. Jones et al. (1989) applied a sectional stress block approach to analyzing beams repaired with epoxy-bonded steel plates, and achieved reasonably good correlations. Shahawy et al. (1995) also employed sectional analysis procedures for analyzing beams strengthened with carbon FRP laminates, and achieved similar success. Kaliakin et al. (1995) used the program ABAQUS to analyze reinforced concrete T-beams enhanced with external FRP overlays. While their analyses fairly accurately captured the overall load-deflection response of the beams, some numerical stability and localization problems were experienced. Advancements were made by Arduini et al. (1997), who, also using ABAQUS, employed a smeared crack approach in modeling RC beams strengthened with FRP plates and flexible sheets. However, these analyses were limited to situations where monotonic loading was applied to beams that had no loading or damage prior to the application of the FRP or steel plates. Going beyond this limitation, Ziraba (1993) reported work in which analyses were performed for elements strengthened after previous loading and damage. A finite-element program was developed that performed nonlinear analyses of FRP-repaired beams subjected to an arbitrary load history prior to repair. The reported correlations with experimental results were generally good with respect to load-deflection responses at intermediate load levels, but numerical instabilities were encountered near ultimate load. Thus, the sum of the work done in this area is not extensive and has met with only limited success. Commercial FEM programs also remain deficient, given their general inability to model shear-critical behavior for reinforced concrete structures.

This paper will present an alternative method for analyzing repaired or retrofitted concrete structures subjected to prior loading and damage. The procedure can be implemented into a nonlinear finite-element algorithm based on a secant stiffness formulation. Significant improvements in modeling capabilities lie in the procedure's ability to incorporate realistic material behavior models in a smeared rotating crack context.

OVERVIEW OF METHODOLOGY

A procedure was previously described by Vecchio (1999) by which nonlinear analyses of reinforced concrete can be made to account for arbitrary loading histories in the context of a secant stiffness formulation. The method was based on defining plastic offset strains for concrete and reinforcement, then enforcing these offsets through the use of prestrain nodal forces. The net elastic strains were then used to define effective secant stiffness factors in formulating the composite stiffness matrix for the reinforced concrete element. The formulation is based on an orthotropic representation of concrete, using a smeared fully-rotating crack model (Vecchio 1989). The resulting procedure was shown to provide a platform for accu-

[1]Prof., Dept. of Civ. Engrg., Univ. of Toronto, 35 St. George St., Toronto, Canada M5S 1A4.

[2]Grad. Student, Dept. of Civ. Engrg., Univ. of Toronto, 35 St. George St., Toronto, Canada M5S 1A4.

Note. Associate Editor: Walter H. Gerstle. Discussion open until November 1, 1999. To extend the closing date one month, a written request must be filed with the ASCE Manager of Journals. The manuscript for this paper was submitted for review and possible publication on August 7, 1998. This paper is part of the *Journal of Structural Engineering*, Vol. 125, No. 6, June, 1999. ©ASCE, ISSN 0733-9445/99/0006-0644–0652/$8.00 + $.50 per page. Paper No. 18964.

rate simulations of reinforced concrete structures to monotonic and cyclic loading conditions.

The plastic offset approach can be used to construct an algorithm enabling the analysis of structures whose details are altered partway through the loading history. This can include situations involving multistage construction, or structures that are repaired, rehabilitated, or retrofitted in some manner. In such cases, it can be of some importance to retain a history of the residual strains or damages that are present in the portions of the structure that remain, rather than assuming in the analysis of the altered structure that all elements revert to a zero stress and zero strain condition. This is particularly significant in in situ structures that have sustained some damage due to extreme loading (such as during an earthquake) but remain in service as the repair is being effected. The proportions of the load shared between remaining original elements and newly constructed portions of the structure are highly dependent on a rigorous consideration of the strain differentials that exist.

The key feature in the analysis procedure proposed is the ability to engage and disengage elements at any time in the loading history. Elements that are initially disengaged experience the same strains that adjoining elements experience, but these strains are retained as plastic offset strains. The elastic components of the strains being imposed on a disengaged element remain at zero; therefore, the element contributes nothing to the strength or stiffness of the structure. When an initially disengaged element is activated partway through a load-history analysis, it begins to contribute to the structural rigidity starting from a zero elastic strain condition. When an initially engaged element is deactivated partway through an analysis (representing a condition where a portion of the structure is removed), the element no longer makes a contribution to the structural stiffness. Thus, a finite-element model representing a rehabilitated or sequentially constructed structure must be double-meshed to some extent. The double sets of elements will be necessary to model portions of the structure that are initially present, portions that are subsequently added, and portions that are subsequently removed.

The analysis approach is schematically summarized in Fig. 1. The situation being modeled is one where a steel or FRP plate is bonded to the soffit of a flexural member after it has been subjected to load and sustained some damage (e.g., cracking or crushing of concrete, or yielding of the reinforcement). The finite-element model is formulated to represent both the initial beam and the plate subsequently added [see Fig. 1(a)]. At the onset of loading [point A in Fig. 1(b)], only those elements representing the original concrete beam are active. At point B in the loading sequence, the elements representing the bonded soffit plate are engaged and become active. At this point, an element from the soffit will have undergone a deformation primarily tensile in nature; this strain is taken as an initial plastic offset strain ε_p, as shown in Fig. 1(c). The plastic offset is then used in calculating the effective secant stiffness for the element [Fig. 1(d)].

The finite-element program used in this work is based on an implementation of the Modified Compression Field Theory (MCFT) (Vecchio 1989, 1990). The constitutive models for the concrete and reinforcement are as previously described for the MCFT (Vecchio and Collins 1986) and represent such second-order mechanisms as compression softening of the concrete, tension stiffening effects in the concrete, crack shear slip, lateral expansion and confinement effects, and Bauschin-

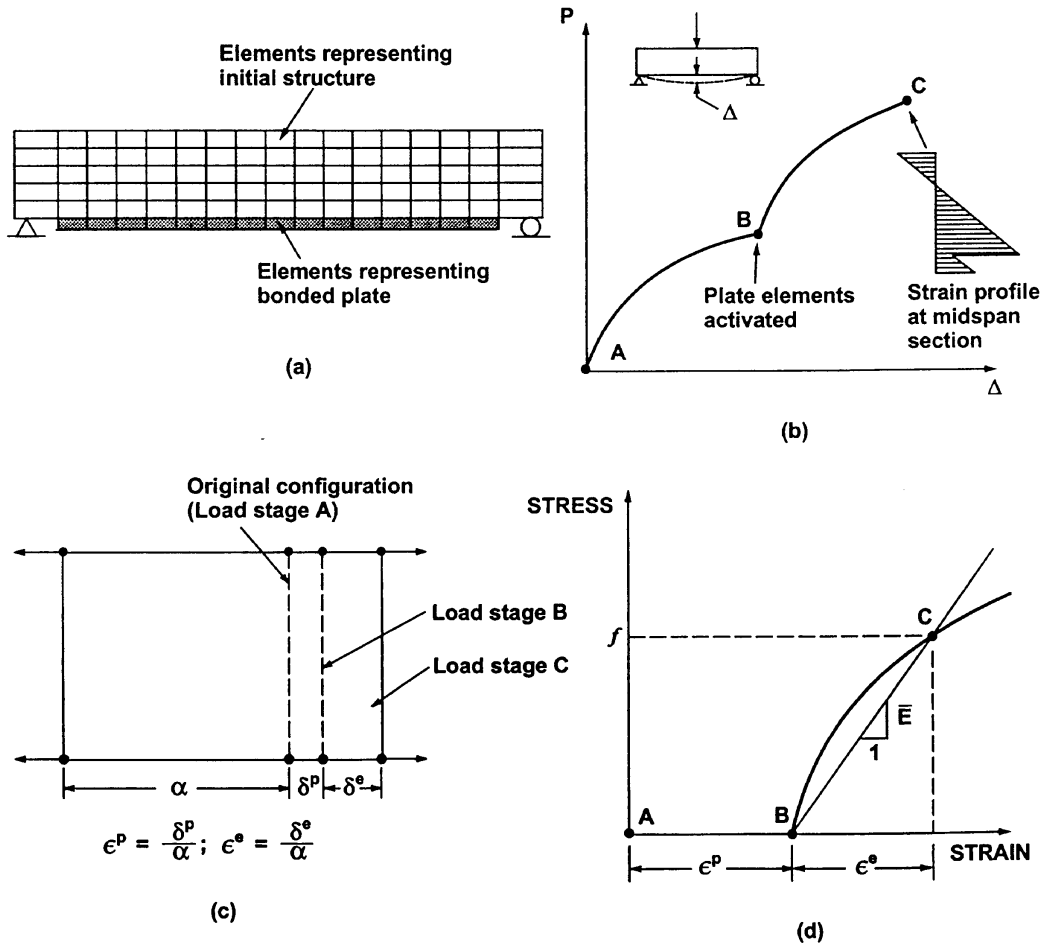

FIG. 1. Analysis of FRP-Repaired Beam: (a) Finite-Element Mesh; (b) Loading History; (c) Strain Conditions in Plate Element; (d) Definition of Secant Modulus

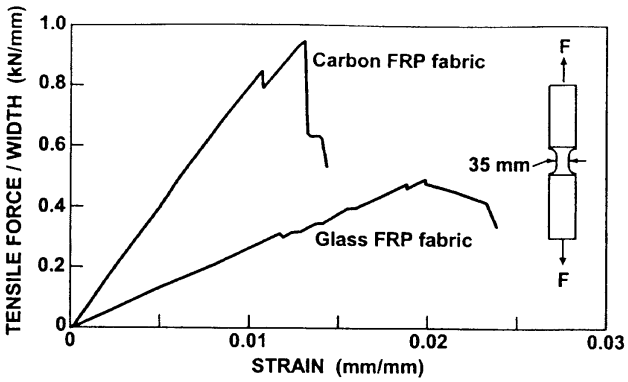

FIG. 2. Typical Tensile Properties of FRP Fabric

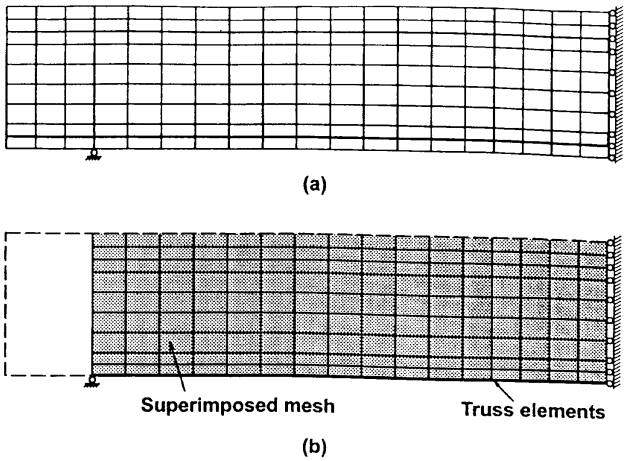

FIG. 4. Finite-Element Model of DeRose Slab Specimens: (a) Elements Representing Initial Structure; (b) Elements Representing FRP Overlays

ger effects in the reinforcement. To represent the behavior of glass and carbon FRP sheets, the constitutive responses illustrated in Fig. 2 were added. Here, it is assumed that the bonding agents add no stiffness. The FRP fibers are assumed to be essentially linear elastic with brittle fracture in tension and ineffective when in compression.

FINITE-ELEMENT FORMULATION

Consider an initially disengaged element that, as an integral part of some structure, is subjected to an arbitrary loading history. The element experiences straining which, in a two-dimensional formulation, is represented by the total strain vector $[\varepsilon]$:

$$[\varepsilon] = \begin{bmatrix} \varepsilon_x \\ \varepsilon_y \\ \gamma_{xy} \end{bmatrix} \tag{1}$$

At the point in loading history where the element is engaged, the total strains present at that time are set equal to a plastic offset strain vector $[\varepsilon_c^p]$. Thus, the initial plastic offsets in the concrete, relative to a global reference axes (x, y), are defined as

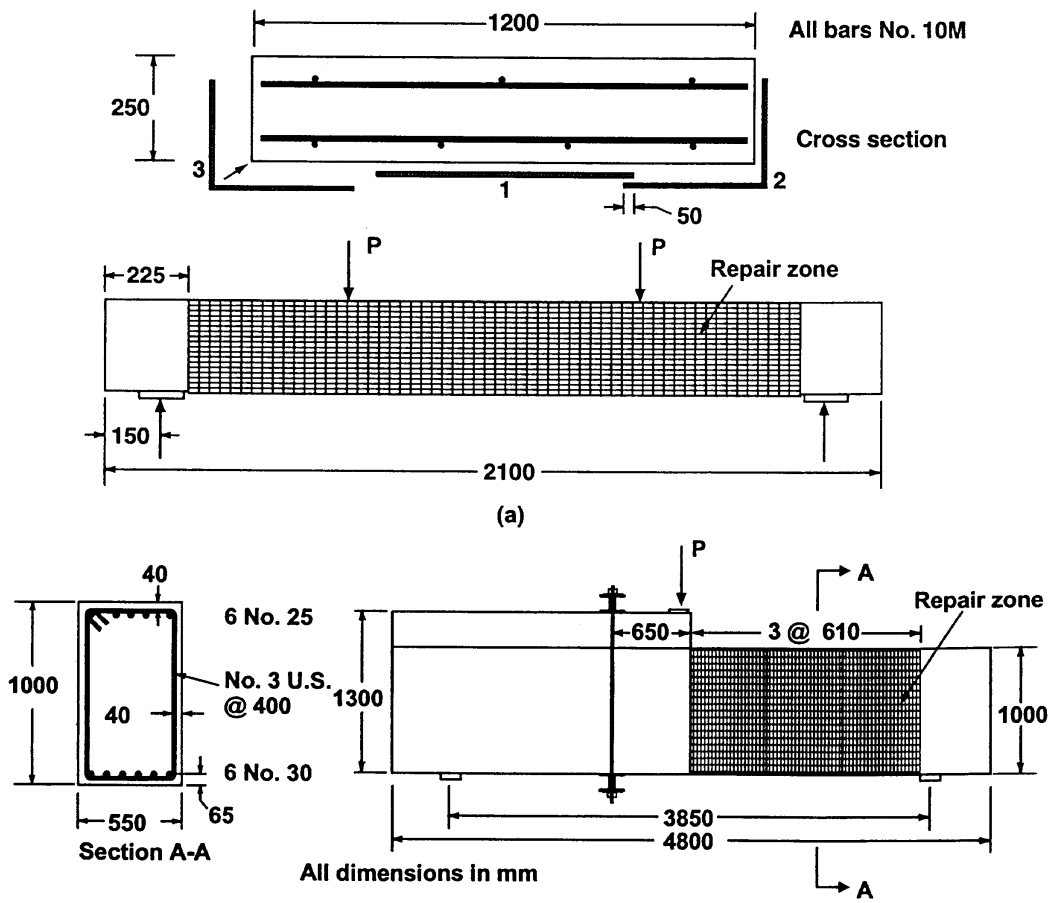

FIG. 3. Details of DeRose Specimens: (a) Slab Specimens; (b) Beam Specimens

$$[\varepsilon_c^p] = \begin{bmatrix} \varepsilon_{cx}^p \\ \varepsilon_{cy}^p \\ \gamma_{cxy}^p \end{bmatrix} \quad (2)$$

From the plastic prestrains, the free joint displacements $[r_c^p]$ are determined as functions of the element geometry, nominally represented by the following:

$$[r_c^p] = \int [\varepsilon_c^p]\, dx \quad (3)$$

Then, given the free displacements, the plastic prestrain nodal forces can be evaluated using the effective element stiffness matrix due to the concrete component:

$$[F_c^p] = [k_c][r_c^p] \quad (4)$$

The force vector due to the plastic offsets is then added to the total load vector. An iterative solution procedure is employed thereafter to effect a nonlinear analysis; the procedure is similar to that previously described for elastic strain offsets (Vecchio 1990, 1992).

Note that in defining the secant stiffness matrix for the concrete material, the stiffnesses are taken with respect to a zero stress-strain point corresponding to the plastic strain offset in each of the principal strain directions. Thus, an elastic strain vector is initially defined by subtracting the plastic strains from the total strains:

$$[\varepsilon_c^e] = [\varepsilon] - [\varepsilon_c^p] \quad (5)$$

The elastic strains are then resolved into principal strains, ε_i. From an appropriate set of constitutive relations (the MCFT

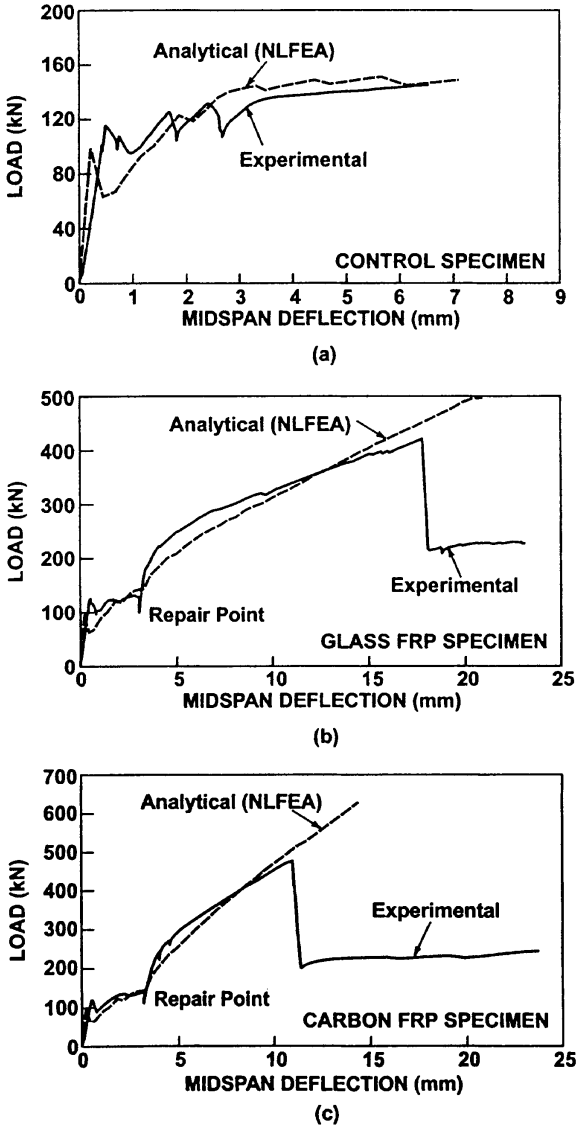

FIG. 5. Comparison of Load-Deflection Responses for DeRose Slab Specimens: (a) Control Slab; (b) Glass FRP-Repaired Slab; (c) Carbon FRP-Repaired Slab

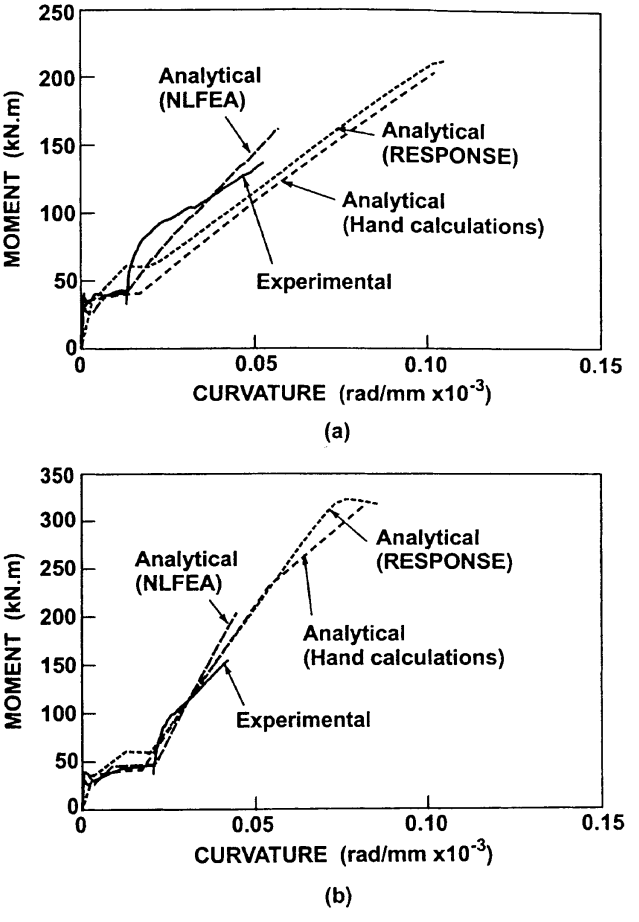

FIG. 6. Moment-Curvature Responses, at Midspan, for DeRose Slab Specimns: (a) Glass FRP-Repaired Slab; (b) Carbon FRP-Repaired Slab

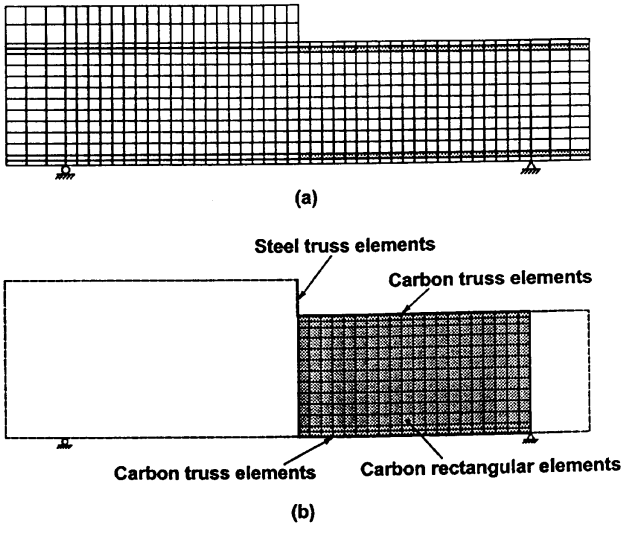

FIG. 7. Finite-Element Model of DeRose Beam Specimens: (a) Elements Representing Initial Structure; (b) Elements Representing FRP Overlays

relationships are used herein), the corresponding principal concrete stresses f_{c_i} are determined. The elastic strains and stresses are then used to compute effective secant stiffness values:

$$\bar{E}_{c_i} = \frac{f_{c_i}}{\varepsilon_{c_i}} \tag{6}$$

Plastic offsets for each of the reinforcement components, in an initially disengaged element, are calculated in a similar manner. Again, the formulation follows a similar development as for elastic offsets; see Vecchio (1990, 1999). In this study, FRP fabric is treated as smeared reinforcement.

Note that measures of the plastic offsets, strain history, and damage must be carried forward in an incremental load analysis. At each load stage, the plastic offset strains are updated as necessary.

CORROBORATION WITH FRP-REPAIRED ELEMENTS

DeRose (1997) tested several slabs and beams repaired with glass and carbon FRP overlays. The tests were unique in that the elements were loaded to an advanced degree of damage, and the load was then held constant while the repairs were made. Following an adequate curing period, loading was resumed and continued until failure. The results from these tests will be used to examine the accuracy of the analysis procedure proposed.

Three simply supported slab specimens, 1,200 × 250 mm in cross section and 2.1 m in length, were tested under two-point loading conditions. The slabs were very lightly reinforced, containing four 10M bottom bars and three 10M top bars in the longitudinal direction. No shear reinforcement was provided. The first slab, taken as the control specimen, was loaded to failure without any repair intervention. It demonstrated a highly ductile behavior, failing in flexure at a load of 193 kN, which was nominally above the cracking load. The second specimen was initially loaded to 135 kN, at which level the longitudinal reinforcement was well into yielding and crack widths were in the range of 0.4 mm. At this point, load was maintained constant, and the soffit and sides of the slab were repaired with carbon FRP fabric. After a three-day curing period, the loading was resumed. The slab was able to sustain a load of 478 kN. Further, the ensuing failure was shear dominant, with the formation of large inclined cracks accompanied by the delamination of the carbon FRP fabric. The third specimen was tested in a similar manner to the second, except that glass FRP was used for the repair. It also failed in shear, at an ultimate applied load of 422 kN. A sketch of the slab details is given in Fig. 3(a); full details are provided by DeRose (1997).

The slab specimens were modeled using the finite-element mesh shown in Fig. 4. A mesh consisting of 171 elements was used to model the initial structure. This was overlaid with an additional mesh consisting of 144 rectangular elements and 16 truss bar elements. (Note: For this and all subsequent analyses described, eight-dof constant strain rectangular elements were used). The rectangular elements represented the glass or carbon FRP subsequently applied to the sides of the slab. The truss bar elements were used to represent the layer of FRP applied to the soffit of the slabs. Analyses were undertaken for each of the three test specimens (control, carbon FRP repaired

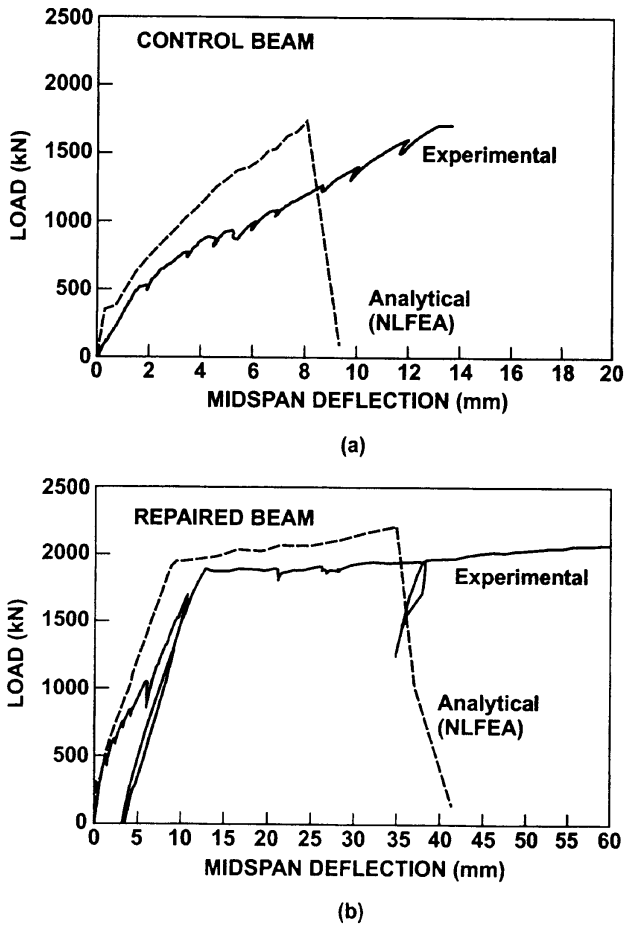

FIG. 8. Load-Deflection Responses for DeRose Beam Specimens: (a) Control Beam; (b) Carbon FRP-Repaired Beam

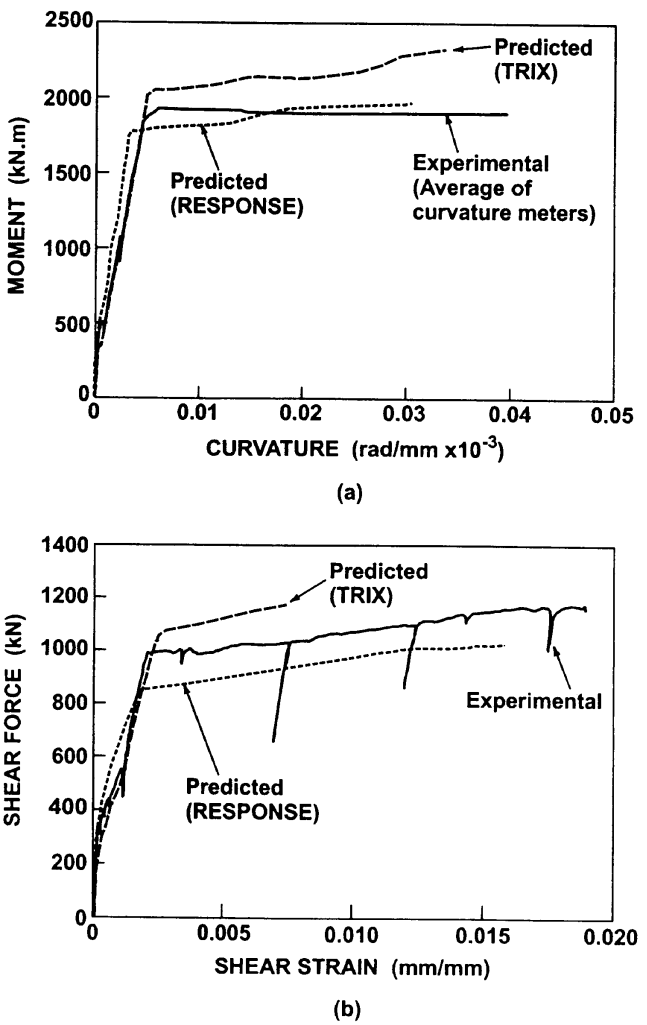

FIG. 9. Sectional Responses for DeRose Beam Specimen: (a) Curvature; (b) Transverse Shear Strains

and glass FRP repaired) to determine their theoretical response to monotonically increasing two-point load as tested. With the latter two specimens, the initially disengaged elements representing the FRP overlays were activated when the computed center deflection reached 3.5 mm, coinciding with the displacements at which the laboratory specimens were repaired. (The analyses were conducted in a displacement-imposed mode, as opposed to load-imposed.)

Compared in Fig. 5 are the predicted and observed load-deflection curves for the three slab specimens. As mentioned, the control specimen was very lightly reinforced (0.15% longitudinal reinforcement) and experienced a ductile yielding failure at loads barely above the cracking load. This behavior was simulated reasonably well in the analysis [see Fig. 5(a)]. The precracking stiffness, postcracking ductility, and peak load were all represented accurately. The two repaired specimens exhibited greatly increased load-carrying capacity, before ultimately experiencing a shear failure. Shown in Figs. 5(b and c) are the observed and predicted responses for the glass and carbon repaired slabs, respectively. The analyses correctly predicted shear failures for the two specimens, marked by excessive straining and strength loss in the concrete, although at loads about 15–20% greater than those actually achieved. The analyses made no attempt to include provisions for modeling the debonding of the FRP sheets, and this may have contributed to the overprediction of strength. Apart from this, all other aspects of the behavior are well represented. Note, in particular, that the changes in stiffness prior to and after repair were simulated accurately. Concrete surface strains, reinforcement strains, and the section shearing strains were also modeled well.

Shown in Fig. 6 are predicted and observed moment-curvature responses for the two repaired slabs at their center-points. The theoretical responses were obtained by various means, including: hand calculations assuming conventional plane sections theory; a computer-based sectional analysis procedure that also accounts for shear effects (the program RESPONSE); and the nonlinear finite-element procedure presented herein. Note that the two sectional procedures result in grossly overestimated strengths, even though the computer-based one, using a layer section analysis also based on the MCFT, ostensibly accounts for shear failure. The nonlinear finite-element procedure provides a relatively more accurate simulation, with further prospects for improvement if debonding actions can be incorporated into the analyses.

DeRose (1997) also tested two haunched deep beams, containing light amounts of vertical (shear) reinforcement and thus designed to be initially critical in shear [see Fig. 3(b)]. The beams were subjected to monotonically increasing center-point loading. The first specimen was loaded to failure without any repair treatment. Several large diagonal cracks developed in the specimen, giving way to a brittle shear failure at a load of

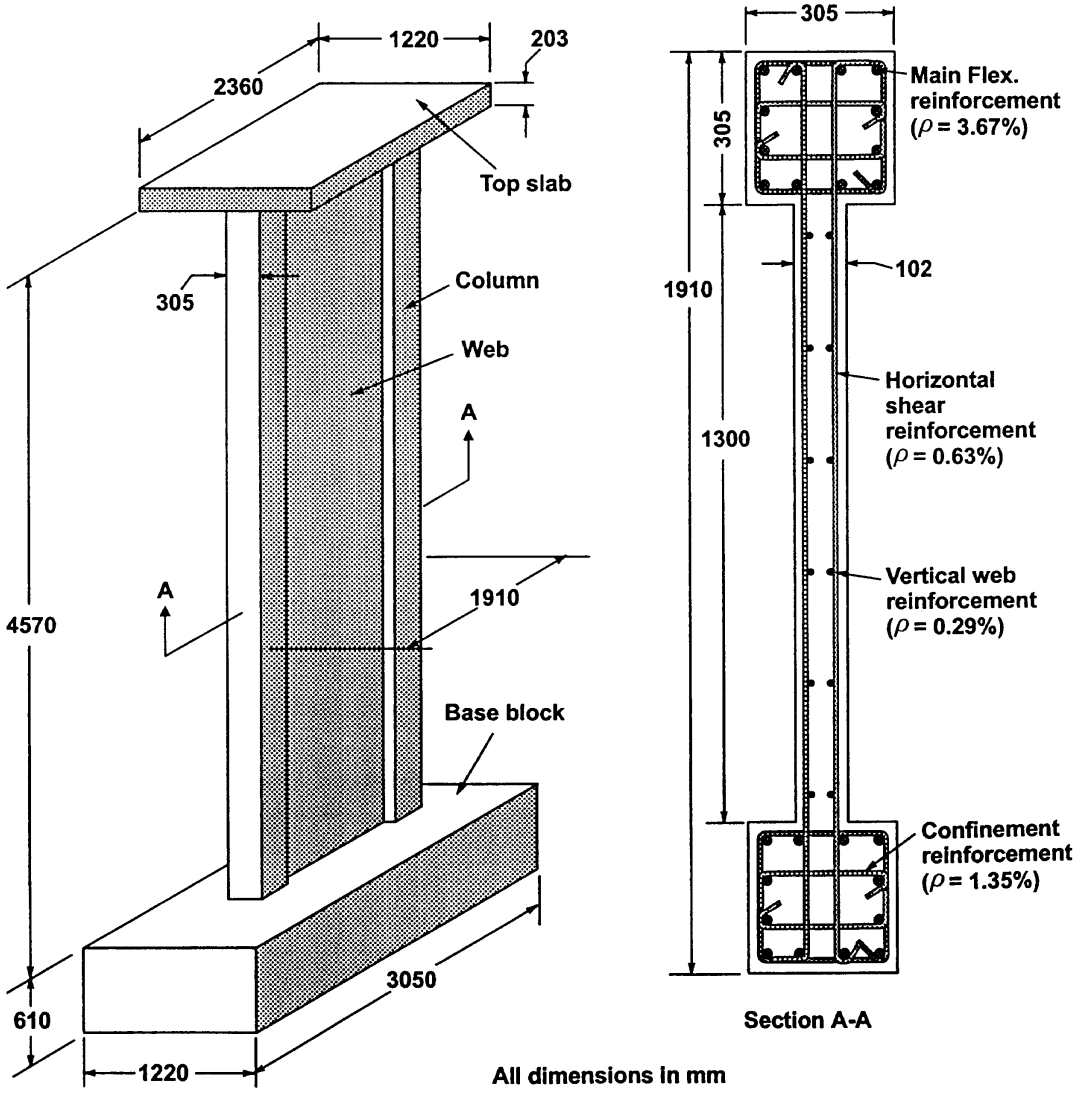

FIG. 10. Details of Shear Wall B5 Tested by Fiorato et al. (1983): (a) Overall Dimensions; (b) Cross Section Details

approximately 1,700 kN. The second specimen was initially loaded to 1,180 kN, at which point five diagonal cracks had formed in the test zone, ranging in width from 0.2 to 0.8 mm. The average strain in the bottom flexural reinforcement was approximately 1.5×10^{-3}, and the structure was showing obvious distress. At this point, the load was held constant while a repair with carbon FRP was carried out. Fabric was applied to the sides, top, and bottom surfaces of the beam in the test region. The load application point was also strengthened with a steel plate and clamping rods. After a three-day curing period for the epoxy bonding agent, loading resumed. The specimen then behaved in a ductile manner, with the flexural reinforcement reaching yield and then strain hardening. The load capacity increased to 2,530 kN, and the deflection capacity increased to 143 mm (compared with 14 mm in the control specimen, see Fig. 8). The final failure, now distinctly flexural in nature, was accompanied by some debonding of the carbon FRP fabric. Again, full details of the test specimens and results are provided by DeRose (1997).

The test beams were modeled in a manner similar to the slabs. The control specimen was represented by 644 rectangular elements, with an additional 286 rectangular elements and 57 truss elements added to account for the repair materials. The mesh used is shown in Fig. 7. Analyses were undertaken by imposing a displacement at the center of the beam. In analyzing the repaired beam, the initially disengaged elements representing the carbon FRP repair materials were activated when the load reached 1,180 kN.

The analysis of the control beam indicated a brittle shear failure, near the right support region, at a load of approximately 1,800 kN. Fig. 8(a) compares the predicted and observed load-deflection responses for the control specimen. While the nonlinear finite-element analysis provides a good estimate of the failure load, the predicted load-deflection response is considerably stiffer both prior to and after first cracking. [Softness in the supports for the test beam may be the cause of the discrepancy, since the procedure has been shown in numerous other investigations to accurately model stiffness in monotonically loaded, nonrepaired beams critical in shear (Vecchio 1989)]. The failure of the carbon FRP-repaired beam was transformed to one governed by a ductile yielding of the main flexural reinforcement. The nonlinear finite-element procedure once again properly captured the change in failure mode and the enhancement in strength, as shown in Fig. 8(b). Again, however, the discrepancies in the stiffness of response are substantial. Shown in Fig. 9 are the curvature and shear strains at a section near the failure zone, about 500 mm from the load application point. Also shown are the corresponding behaviors predicted by the nonlinear finite-element procedure and by the sectional analysis program (RESPONSE). The nonlinear finite-element analysis provides close simulations of the sectional behavior, contradicting the discrepancies noted in the midspan deflection response. Note too that the test beam exhibited more ductility than predicted. In beams containing little or no shear reinforcement and failing in a flexural-shear mode, ductility is highly dependent on aggregate interlock and shear slip models, and can show considerable variation.

CORROBORATION WITH CYCLICALLY LOADED SHEAR WALL

Fiorato et al. (1983) reported on a series of large-scale shear walls that were subjected to cyclic loading, tested to advanced stages of damage, repaired by reconstructing the damaged elements, and retested. One of the shear walls tested will be examined here. This will test the ability of the analysis pro-

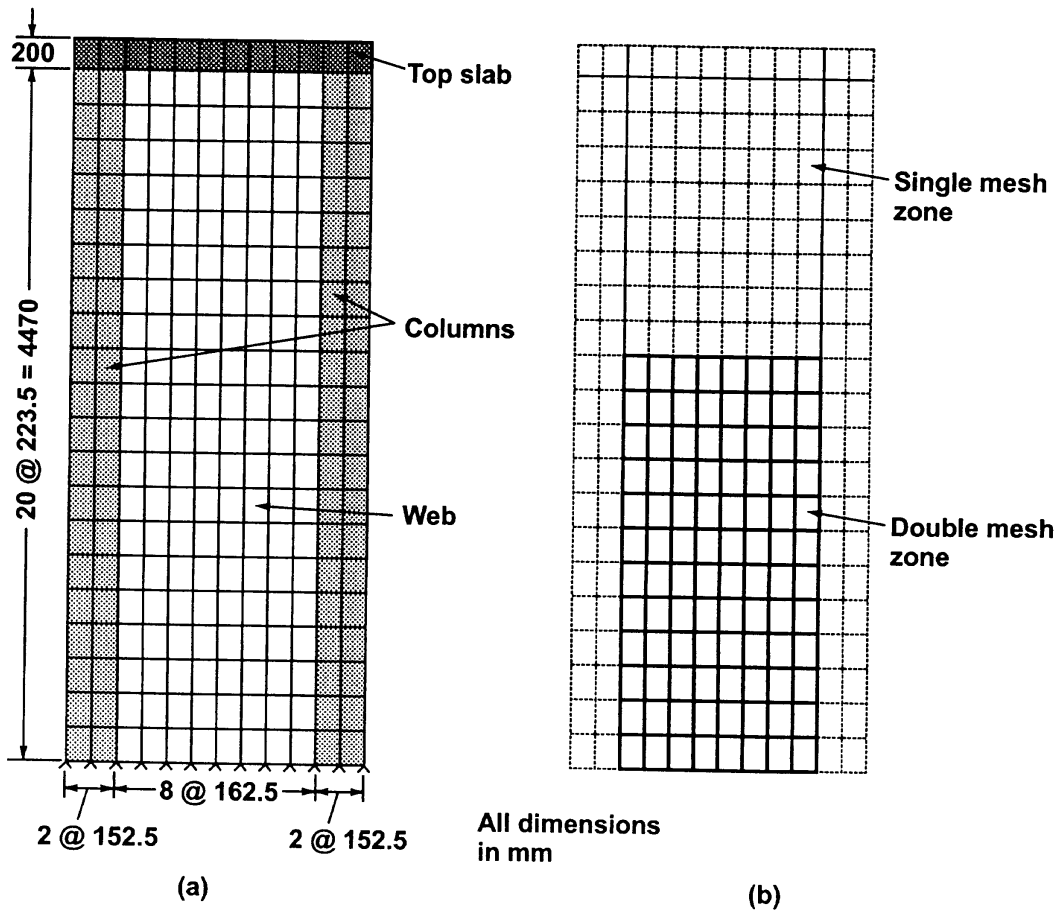

FIG. 11. Finite-Element Model of Wall B5: (a) Elements Representing Initial Structure; (b) Elements Representing Replaced Wall

cedure to model structures where the repair measure involves removing heavily damaged elements and rehabilitating with new or enhanced elements. Also, modeling under the more severe condition of cyclic loading will be tested.

The shear wall chosen for investigation was Specimen B5, a flanged shear wall, with heavily reinforced confined columns framing the outside edges of web element. Wall section details are provided in Fig. 10. The wall was subjected to reversing cyclic lateral loads applied at the top slab level. The loading history was such as to essentially impose displacement cycles in increments of 25 mm (1 in.) amplitude, with three complete cycles at each amplitude level. Specimen B5 was able to sustain two cycles at 125 mm (5 in.) amplitude, before showing significant decay in strength and stiffness during the third cycle. The authors reported that the web of Specimen B5 was completely destroyed during the test, but the columns remained in good condition. The concrete cover had spalled off near the base of the wall at the compression face of each column, but the confined cores were intact. No main flexural reinforcing steel had fractured or buckled, but strains in the column reinforcement had progressed to about 10 times the yield strain. The repair procedure chosen was to completely remove and replace the web concrete to a level above the midheight of the wall. The reinforcing steel was left intact, and no new steel was added. Also, several areas near the base of the columns, where the outer shell concrete had crushed, were repaired. The shear wall, redesignated as Specimen B5R, was retested according to the same loading regime as the original wall. (See Fiorato et al. (1983) for full details.)

This wall was modeled using the finite-element mesh shown in Fig. 11. A total of 252 rectangular elements were used to represent the original wall. The bottom portion of the wall was double-meshed with an additional 96 rectangular elements to represent the new concrete web installed later. An analysis was undertaken of B5 by imposing displacements in the pattern used during the test. At the end of the second cycle at ± 125 mm (5 in.), the elements representing the lower portion of the web (to a height of 2.6 m above the base) were disengaged, and the new web elements were activated. (At this point in the analysis, the reinforcement at the base of the columns had average residual strains of about 25.0×10^{-3}. Crack widths at the column bases were in the range of 2.0 mm, and the elongation of the columns and web resulted in a total vertical displacement at the top slab of about 30.0 mm. These strain and damage conditions were inherently carried forward in the plastic offsets and other strain measures previously discussed.) The analyses then recommenced tracing the displacement history applied previously. Note that no attempt was used to model the concrete repaired in the columns, although this could have been done with some additional meshing. Also note that the cyclic analyses are based on constitutive models described by Vecchio (1999), which are preliminary in nature. These models do not, as yet, completely account for progressive damage in cyclically loaded concrete.

Shown in Figs. 12(a and b) are the experimentally observed load-deflection responses for the original and repaired walls, respectively. Fiorato et al. (1983) point out that the repair procedure implemented was fairly effective. The strength and de-

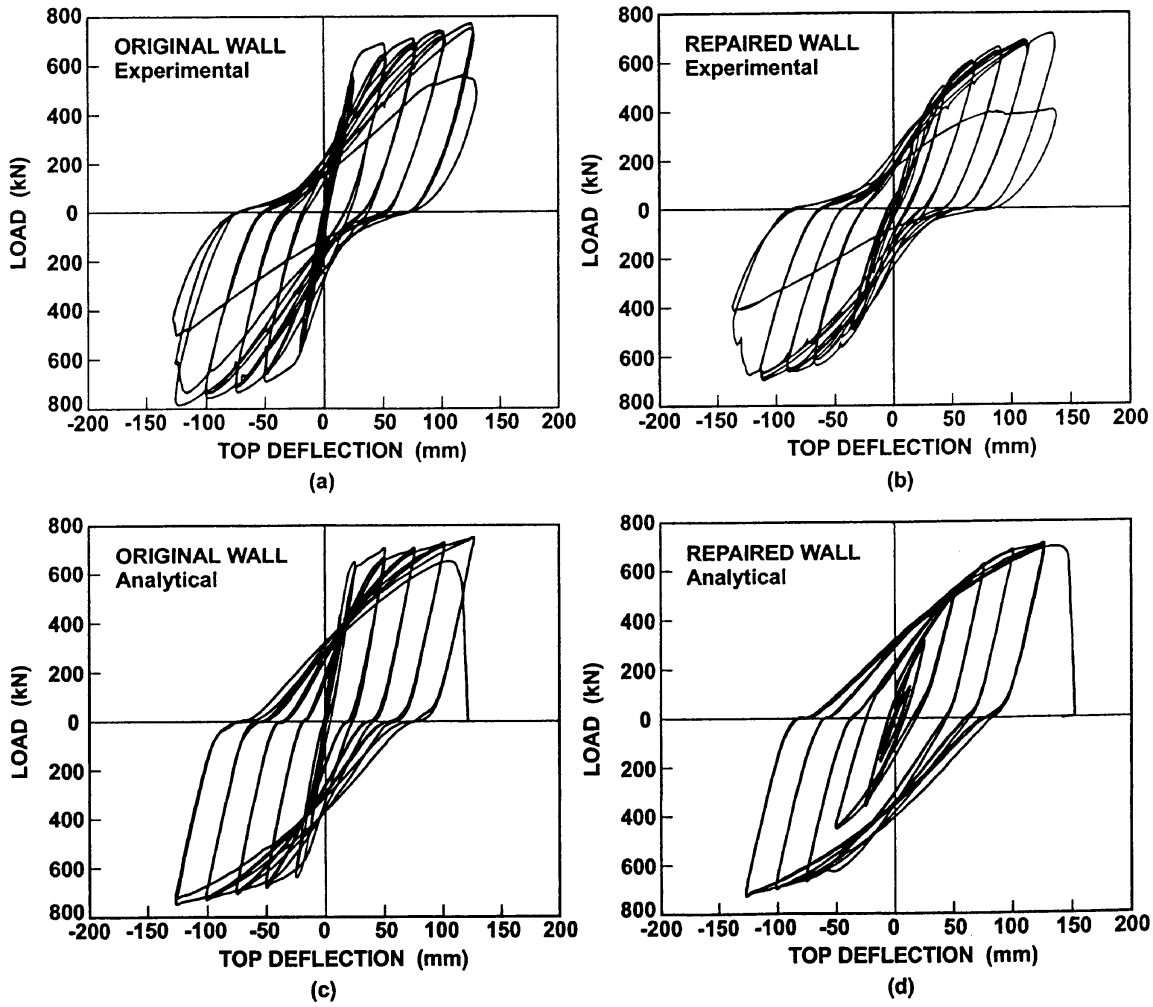

FIG. 12. Load-Deflection Responses of Wall B5: (a) Measured Response of Original Wall; (b) Measured Response of Repaired Wall; (c) Computed Response of Original Wall; (d) Computed Response of Repaired Wall

formation capacity of the wall were reinstated to original levels. However, the initial stiffness of the repaired wall was only about 50% that of the original wall. Interestingly, the repaired wall was able to withstand more deformation than the original wall, maintaining its integrity into the second cycle at 150 mm (6 in.) displacement. Shown in Figs. 12(c and d) are the computed load-deflection responses for the original and repaired walls, respectively. For the original wall, the strength and deformation response is reasonably well predicted, with failure occurring during the third cycle at 125 mm (5 in.) displacement, as observed in the test. The predicted response is marginally stiffer than observed, however. Also, the predicted response has a somewhat flatter load plateau; Fioato et al. (1983) did not provide a value for the strain hardening modulus of the reinforcement, and so a relative low value of 2,000 MPa was assumed. Otherwise, the ultimate load capacity, deformation response, and failure mode are accurately captured. The response of the repaired wall is also well simulated. The initial stiffness is somewhat underestimated, likely due to the fact that the localized repairs applied to the concrete at the base of the columns were not modeled. Otherwise, as the loading progressed, the strength and stiffness response was well captured in the analyses. Failure was predicted to occur during the first positive cycle at 150 mm (6 in.), again matching the experimental results.

CONCLUSIONS

It is possible to implement modifications to nonlinear finite-element procedures that will enable the analysis of repaired, retrofitted, or sequentially constructed concrete structures. The method presented uses the concept of plastic strain offsets, coupled with the provision to engage and disengage elements at various stages of loading. Material models realistically representing the nonlinear behavior of concrete, reinforcement, and various repair materials are easily incorporated. The resulting procedure is numerically stable and efficient, and it is adaptable to many practical situations.

The procedure was used to simulate the response of a series of glass and carbon FRP-repaired beams and slabs. It was shown to provide reasonably accurate representations of the changes in strength, stiffness, ductility, and failure mode. Shear-critical and flexure-critical failure mechanisms were equally well represented. The finite-element analyses provided considerably more accurate simulations of the repaired structures than could be obtained from hand or computer-based sectional analysis procedures.

The analysis of a repaired shear wall subjected to reversed cyclic loads demonstrated the procedure's ability to model severely damaged structures in which portions must be removed and reconstructed. In the portions remaining, previous load history and damage sustained were significant factors, impacting on the observed response of the repaired structure. These load history effects were successfully carried forward in the reanalysis of the repaired wall.

The analysis procedure described presents a viable means of analyzing the adequacy of various repair scenarios, and in assessing the safety and performance of damaged or otherwise deficient structures before and after rehabilitation. Improvements to the analysis capability can be made by implementing a bond break element to model delamination of repair fabrics or plates. Additionally, for cyclically loaded elements, a cyclic damage model is necessary to fully represent the decay in strength and stiffness of the concrete elements. Work is progressing with respect to both these needs.

APPENDIX I. REFERENCES

Arduini, M., DiTommaso, A., and Nanni, A. (1997). "Brittle failure in FRP plate and sheet bonded beams." *ACI Struct. J.*, 94(4), 363–370.

DeRose, D. (1997). "The rehabilitation of a concrete structure using fibre reinforced plastics," MASc thesis, University of Toronto, Toronto.

Fiorato, A. E., Oesterle, R. G., and Corley, W. G. (1983). "Behavior of earthquake resistant structural walls before and after repair." *ACI Struct. J.*, 80(5), 403–413.

Jones, R., Swamy, R. N., and Charif, A. (1989). "The effect of external plate reinforcement on the strengthening of structurally damaged RC beams." *The Struct. Engr.*, 67(3), 45–56.

Kaliakin, V. N., Chajes, M. J., and Januszka, T. F. (1995). "Analysis of concrete beams reinforced with externally bonded woven composite fabrics." *Proc., 2nd Int. Conf. for Composites Engrg.*, International Community on Composites Engineering, New Orleans, 27(3), 235–244.

Shahawy, M. A., Arockiasamy, M., Beitelman, T., and Sowrirajan, R. (1995). "Analysis of concrete beams reinforced with externally bonded woven composite fabrics." *Proc., 2nd Int. Conf. for Composites Engrg.*, International Community on Composites Engineering, New Orleans, 27(3), 225–233.

Vecchio, F. J. (1989). "Nonlinear finite element analysis of reinforced concrete membranes." *ACI Struct. J.*, 86(1), 26–35.

Vecchio, F. J. (1990). "Reinforced concrete membrane element formulations." *J. Struct. Engrg.*, ASCE, 116(3), 730–750.

Vecchio, F. J. (1992). "Finite element modelling of concrete expansion and confinement." *J. Struct. Engrg.*, ASCE, 118(9), 2390–2406.

Vecchio, F. J. (1999). "Towards cyclic load modelling of reinforced concrete." *ACI Struct. J.* (in press).

Vecchio, F. J., and Collins, M. P. (1986). "The modified compression field theory for reinforced concrete elements subjected to shear." *ACI J.*, 83(2), 219–231.

Ziraba, Y. N. (1993). "Nonlinear finite element analysis of reinforced concrete beams repaired by plate bonding," PhD thesis, King Fahd University of Petroleum and Minerals, Dahran, Saudi Arabia.

APPENDIX II. NOTATION

The following symbols are used in this paper:

$\bar{E}_{c_i}$ = secant modulus of concrete in principal direction i;
$[F_c^p]$ = concrete plastic offset joint forces;
f_{c_i} = stress in concrete in principal direction i;
$[k_c]$ = concrete element stiffness matrix;
$[r_c^p]$ = free joint displacements due to concrete plastic offsets;
$[\varepsilon]$ = total strain matrix;
ε_{c_i} = strain in concrete in principal direction i;
$[\varepsilon_c^e]$ = concrete elastic strain matrix;
$[\varepsilon_c^p]$ = concrete plastic strain matrix; and
ρ = percentage of reinforcement.